De Martino, A., Egger, R. & Tsvelik, A. M. (2006). Nonlinear magnetotransport in interacting chiral nanotubes.. Physical Review Letters (PRL), 97(7), . doi: 10.1103/PhysRevLett.97.076402 <http://dx.doi.org/10.1103/PhysRevLett.97.076402>

CITY UNIVERSITY LONDON

EST 1894

City Research Online

Original citation: De Martino, A., Egger, R. & Tsvelik, A. M. (2006). Nonlinear magnetotransport in interacting chiral nanotubes.. Physical Review Letters (PRL), 97(7), . doi: 10.1103/PhysRevLett.97.076402 <http://dx.doi.org/10.1103/PhysRevLett.97.076402>

Permanent City Research Online URL: http://openaccess.city.ac.uk/1663/

Nonlinear magnetotransport in interacting chiral nanotubes

A. De Martino,[1] R. Egger,[1] and A.M. Tsvelik[2]

[1] *Institut für Theoretische Physik, Heinrich-Heine-Universität, D-40225 Düsseldorf, Germany*
[2] *Department of Condensed Matter Physics and Materials Science,*
Brookhaven National Laboratory, Upton, New York 11973-5000, USA
(Dated: March 17, 2011)

Nonlinear transport through interacting single-wall nanotubes containing a few impurities is studied theoretically. Extending the Luttinger liquid theory to incorporate trigonal warping and chirality effects, we derive the current contribution I_e *even* in the applied voltage V and *odd* in an orbital magnetic field B, which is non-zero only for chiral tubes and in the presence of interactions.

Electronic transport experiments on individual single-wall carbon nanotubes (SWNTs) [1] have revealed ample evidence for the Luttinger liquid (LL) phase of one-dimensional (1D) interacting metals induced by electron-electron (e-e) interactions. In its simplest form, the effective low-energy theory for interacting SWNTs [2] is insensitive to the chiral angle θ [3, 4] describing the wrapping of the graphene sheet. This fact can be rationalized by noting that, to lowest order in a $\mathbf{k} \cdot \mathbf{p}$ scheme, the graphene dispersion reflects an isotropic Dirac cone around each K point in the first Brillouin zone [3]. Imposing periodic boundary conditions around the SWNT circumference slices this cone and gives identical dispersion for all θ, as long as the SWNT stays metallic. Such an approach is however insufficient for a description of the magnetotransport effects in chiral tubes. Therefore, we extend the theory [2] to include chirality effects by taking into account trigonal warping, tube curvature, and magnetic field B, and then compute the *nonlinear* two-terminal magnetoconductance. While the well-known Onsager symmetry $G(B) = G(-B)$ [5] excludes linear-in-B terms in the linear conductance, such terms can appear out of equilibrium [6, 7, 8], with first experimental observations reported for SWNTs [9, 10] and semiconductor quantum dots or rings [11, 12, 13, 14, 15].

The current contribution I_e *odd* in B and *even* in the voltage V is of fundamental and unique importance, mainly due to two reasons. First, it requires a *noncentrosymmetric (chiral) medium*, with the sign of I_e depending on the handedness (enantioselectivity) [6], since the current density is a polar vector but magnetic field an axial one. Thus $I_e \neq 0$ requires the simultaneous breaking of time reversal symmetry (by the magnetic field) and of inversion symmetry (by the chiral medium). Second, standard arguments based on the Landauer-Büttiker scattering formalism valid in the noninteracting case [7, 8] show that $I_e \neq 0$ also requires *interactions*. At low temperature (T), e-e interactions should therefore contribute to I_e in leading order. Measurements of I_e probe interactions and chirality in a very direct manner, potentially allowing for the structural characterization of chiral ($\sin 6\theta \neq 0$) interacting nanotubes via transport experiments. Nonetheless, apart from the classical phonon-dominated high-T regime [7], no predictions specific to SWNTs have been made so far. Here we determine the current contribution $I_e(V, T)$ linear in the parallel orbital magnetic field B (Zeeman fields play no role here), for SWNTs in good contact to external leads. The simplest case allowing for $I_e \neq 0$ is found when including at least two (weak) elastic scatterers, representing either defects or residual backscattering induced by the two contacts. Our theory includes the often strong e-e interactions using the bosonization method [16], and holds for arbitrary chiral angle θ. Interactions are characterized by the LL parameter $K \leq 1$ in the charge sector, see Eq. (6) below, with typical estimate $K \approx 0.2$ [2]. Our result for I_e, see Eqs. (9) and (12), is non-zero only for chiral ($\sin 6\theta \neq 0$) interacting ($K < 1$) SWNTs, and changes sign for different handedness ($\theta \to -\theta$). We predict oscillatory behavior of I_e as a function of bias voltage, where the oscillation period depends on the Luttinger parameter K, see Eq. (15). The coefficient [10]

$$\alpha(T) = \lim_{V \to 0} \frac{I_e(V, T)}{V^2 B} \qquad (1)$$

is shown to exhibit power-law scaling at $T \to 0$, with a negative exponent that is again determined by K. Including only elastic impurity backscattering, $\alpha(T)$ does not change sign with T for otherwise fixed parameters.

Chirality effects in the low-energy theory come about when one includes trigonal warping in the band structure. Its main effect is to introduce different Fermi velocities $v_{r\alpha}$ [17] for right- and left-moving excitations ($r = R/L = \pm$) around the two distinct K points ($\alpha = \pm$). All these velocities coincide when disregarding trigonal warping, and in a nominally metallic SWNT are given by $v_{r\alpha} = v = 8 \times 10^5$ m/sec. For clarity, we consider an electron-doped SWNT with equilibrium chemical potential $\mu \equiv \hbar v k_F > 0$ well inside the conduction band, and omit the valence band. Including the trigonal warping to lowest nontrivial order [3, 7], we find

$$
\begin{aligned}
v_{r\alpha} =\ & v \sqrt{1 - \frac{k_{\perp\alpha}^2}{k_F^2}} \Bigg(1 + \alpha \cos 3\theta \frac{k_{\perp\alpha} a}{4\sqrt{3}} \frac{3 - 2k_{\perp\alpha}^2/k_F^2}{1 - k_{\perp\alpha}^2/k_F^2} \\
& - r\alpha \sin 3\theta \frac{k_F a}{2\sqrt{3}} \sqrt{1 - \frac{k_{\perp\alpha}^2}{k_F^2}} \Bigg).
\end{aligned}
\qquad (2)
$$

The effects of tube curvature and magnetic field enter via the quantized transverse momenta

$$k_{\perp\alpha}R = n - \alpha\nu/3 + \Phi/\Phi_0 + \alpha c \cos(3\theta), \qquad (3)$$

where $a = 0.246$ nm is the lattice spacing, R the tube radius, $\Phi = \pi R^2 B$, $\Phi_0 = h/e$ the flux quantum, and the tube curvature results in $c = \kappa a/R$ with $\kappa \approx 1$ [3]. Here integer n with $|k_{\perp\alpha}| < k_F$ are allowed; we focus on the lowest band $n = 0$ in what follows. The index ν distinguishes nominally metallic ($\nu = 0$) and semiconducting ($\nu = \pm 1$) SWNTs, and for simplicity, from now on we assume $\nu = 0$. However, with minor modifications, our theory below also applies to strongly doped semiconducting tubes. We mention in passing that chirality effects are also important for other physical quantities. In particular, scattering by a long-range potential in metallic SWNTs depends on chirality [18, 19].

In terms of annihilation fermion operators $R_{\alpha\sigma}(x)$ and $L_{\alpha\sigma}(x)$ for right- and left-movers of spin $\sigma = \pm$, respectively, the usual linearization of the band structure around the Fermi points then yields $H = H_{LL} + V_{dis}$ (we set $\hbar = k_B = 1$),

$$H_{LL} = -i\sum_{\alpha\sigma} \int dx \left(v_{R\alpha} R_{\alpha\sigma}^\dagger \partial_x R_{\alpha\sigma} - v_{L\alpha} L_{\alpha\sigma}^\dagger \partial_x L_{\alpha\sigma} \right)$$
$$+ \frac{V_0}{2} \int dx \left(R^\dagger R + L^\dagger L \right)^2, \qquad (4)$$

$$V_{dis} = \int dx\, U(x) \left(e^{-2ik_F x} R^\dagger L + \text{h.c.} \right), \qquad (5)$$

where $4V_0/\pi v = K^{-2} - 1$ describes e-e forward scattering interactions [20], and $\alpha\sigma$ summations are implied when not given explicitly. Elastic disorder leads to V_{dis}, e.g., due to impurities, defects or substrate inhomogeneities. We keep only the intra-band backscattering potential $U(x)$, which yields the dominant impurity effect [2]. This Hamiltonian can be efficiently treated by (Abelian) bosonization [16]. Introducing four bosonic fields $\phi_i(x)$ and their dual $\theta_i(x)$, with $i = (c+, c-, s+, s-)$ denoting the total/relative charge/spin modes, the clean Hamiltonian for $v_{r\alpha} = v$ is [2]

$$H_{LL}^{(0)} = \frac{u_c}{2} \int dx \left[K^{-1}(\partial_x \phi_{c+})^2 + K(\partial_x \theta_{c+})^2 \right]$$
$$+ \frac{u_n}{2} \sum_{i \neq c+} \int dx \left[(\partial_x \phi_i)^2 + (\partial_x \theta_i)^2 \right], \qquad (6)$$

where $u_c = v/K$ is the plasmon velocity for the $c+$ mode, and $u_n = v$ for the three neutral modes. Including the $v_{r\alpha}$ differences in Eq. (2) then brings about two new features, acting separately in the decoupled charge ($i = c\pm$) and spin ($i = s\pm$) sectors: (i) couplings between total ($+$) and relative ($-$) modes, and (ii) couplings between mutually dual (θ_i, ϕ_i) fields. The first leads to tiny quantitative corrections but no qualitative changes and is neglected henceforth. Point (ii) is crucial, however, since it implies different velocities ($u_{c,R/L}$ and $u_{n,R/L}$) for right-

and left-moving plasmons. This eventually produces the current contribution I_e in the presence of impurities. To linear order in B, we find

$$u_{c,R/L}/v = 1/K \pm \delta, \quad u_{n,R/L}/v = 1 \pm \delta, \qquad (7)$$
$$\delta = \frac{\Phi/\Phi_0}{2\sqrt{3}k_F R}(a/R)^2 \sin(6\theta).$$

Note that $\delta \neq 0$ requires both $B \neq 0$ and chirality, $\sin 6\theta \neq 0$. Moreover, δ has opposite sign for opposite handedness. It essentially describes the difference of R/L-moving velocities, and depends linearly on B.

Next we address the computation of $I_e(V, T)$, where the current operator is $(2e/\sqrt{\pi})\partial_t \phi_{c+}$. An important point concerns the inclusion of the applied voltage V in a two-terminal setup. For weak impurity backscattering $U(x)$, it is sufficient to address the clean case with adiabatically connected leads, where a time-dependent shift arises [21], $\phi_{c+} \to \phi_{c+} + eVt/\sqrt{\pi}$. However, with chiral asymmetry, $v_R \neq v_L$, there is an additional effect [22] due to the different density of states $\nu_{R/L} = 2/\pi v_{R/L}$ for R/L movers. Starting from the equilibrium chemical potential μ, when applying a voltage, the chemical potentials $\mu_{R/L}$ of R/L movers are set by the left/right reservoirs, respectively, where $\mu_R - \mu_L = eV$. Relative to the equilibrium density, R/L movers are thereby injected with density $\rho_{R/L}^0 = \nu_{R/L}(\mu_{R/L} - \mu)$. We may now write $\mu_{R/L} = \mu + \Delta\mu \pm eV/2$, where $\Delta\mu$ is determined by the condition that in an adiabatically connected impurity-free quantum wire, no charge can accumulate in the steady state [21], $\rho_R^0 + \rho_L^0 = 0$. This yields $\Delta\mu = \delta eV/2$, where $\delta = (v_R - v_L)/(v_R + v_L)$ has been specified in Eq. (7), implying the voltage-dependent shift

$$k_F \to k_F + \delta eV/2v_0, \quad v_0 = \frac{2v_R v_L}{v_R + v_L} = v(1 - \delta^2) \quad (8)$$

in Eq. (5). Under the non-equilibrium Keldysh formalism, to second order in $U(x)$, I_e then follows as

$$I_e = -\frac{2eK}{(\pi a)^2} \int_{-\infty}^{\infty} dt \int dX dx \sin(2k_F x) \qquad (9)$$
$$\times\, U(X + x/2)\, U(X - x/2)$$
$$\times\, \cos(eV[t + \delta x/v_0])\, \text{Im}\, e^{i\pi\mathcal{G}^<(x,t)},$$

where $\mathcal{G}^<$ is the sum of the lesser Green's functions for the four plasmonic modes, see Eq. (11) below.

As a function of time, $e^{i\pi\mathcal{G}^<(x,t)}$ has singularities only in the lower-half complex plane, and therefore $I_e = 0$ for $V = 0$. By inspection of Eq. (9), we also observe that $I_e(-\delta) = -I_e(\delta)$. With Eq. (7) we conclude that I_e is *odd* both in magnetic field and chiral angle. In fact, I_e is the only odd-in-B contribution, since the odd-in-V part of the current turns out to be *even* in B. We can now state a first necessary condition for $I_e \neq 0$, namely $\delta \neq 0$, which requires the simultaneous breaking of time reversal and inversion symmetry. Approximating the impurity

potential as $U(x) = \sum_i U_i \delta(x - x_i)$, Eq. (9) becomes

$$I_e = -\frac{4eK}{(\pi a)^2} \sum_{j>k} U_j U_k \sin(2k_F x_{jk}) \quad (10)$$

$$\times \int dt \cos(eV[t + \delta x_{jk}/v_0]) \, \mathrm{Im} \, e^{i\pi \mathcal{G}^<(x_{jk},t)}$$

with $x_{jk} = x_j - x_k$. Then a second necessary condition arises: there should be just a few impurities. The function $\mathcal{G}^<(x,t)$ changes slowly on the scale k_F^{-1}, and when one has to sum over many impurities, $I_e = 0$ due to the fast oscillations of $\sin(2k_F x_{jk})$ in Eq. (10). In such a disordered case, however, *fluctuations* exhibit related magnetochiral transport effects [8]. When only a few impurities (but at least two) are present, there is no averaging and the effect survives in the current, albeit its magnitude and sign are of course sample-dependent. It is likely that the experiments of Ref. [10] were performed on samples with not too many impurities, for otherwise strong localization effects characteristic for 1D systems would render them insulating. Below we focus on the simplest case of two impurities separated by a distance $L = x_2 - x_1$, see also Ref. [23]. Such a controlled two-impurity setup can be experimentally realized in individual SWNTs [24].

As further evaluation of Eq. (10) requires numerical integration routines, we first examine the spinless single-band version of Eq. (4), which contains the essential physics and allows to compute I_e in closed form [25]. Given the Fermi velocities $v_{r=R/L=\pm} = v(1 \pm \delta)$ [corresponding to Eq. (2)], the plasmon velocities of the clean interacting system are $u_{R/L} = v(1/K \pm \delta)$ [corresponding to Eq. (7)]. The plasmon lesser Green's function is

$$G^<(x,t) = \frac{iK}{4\pi} \sum_r \ln \left[\frac{u_r}{\pi aT} \sinh \left(\frac{\pi T}{u_r}[x - ira - ru_r t] \right) \right].$$
$$(11)$$

Using $2u_R u_L/(u_R + u_L) \simeq v/K$, some algebra yields

$$I_e = \frac{2eK^2}{\pi L} \frac{U_1 U_2}{v} (a/L)^{2K-2} \sin(2k_F L) \, \tilde{T}^{2K-1} e^{-K\tilde{T}}$$

$$\times \sin[\delta(1 - K^2)\tilde{V}/K] \, \mathrm{Im} \left[\frac{\Gamma(1 + K - i\tilde{V}/\tilde{T})}{\Gamma(K)\Gamma(2 - i\tilde{V}/\tilde{T})} \right. \quad (12)$$

$$\left. \times \, e^{i\tilde{V}} F\left(K, 1 + K - i\tilde{V}/\tilde{T}; 2 - i\tilde{V}/\tilde{T}; e^{-2\tilde{T}}\right) \right],$$

where Γ is the Gamma function and F the hypergeometric function [26]. We introduced dimensionless temperature and voltage

$$\tilde{T} \equiv \frac{2\pi k_B T}{\hbar v/(KL)}, \quad \tilde{V} \equiv \frac{|eV|}{\hbar v/(KL)}. \quad (13)$$

Obviously, $I_e = 0$ in the noninteracting case ($K = 1$), and thus interactions provide a third necessary condition for $I_e \neq 0$. Equation (12) now allows to analyze
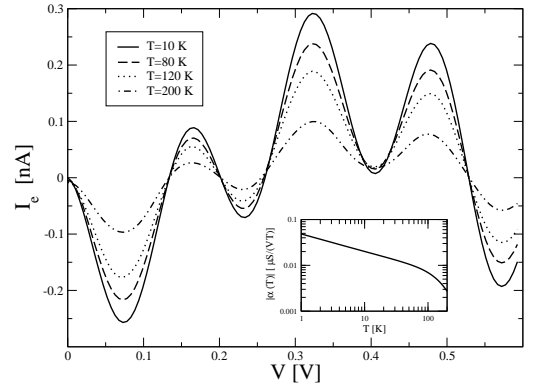

FIG. 1: Even-in-voltage part of the current I_e (in nA) as a function of bias voltage (in V) for several temperatures. Results are shown for a $(10,4)$ SWNT with $K = 0.23$, $B = 16$ T, containing two impurities ($L = 20$ nm, $U_{1,2} = v/2$). Inset: Coefficient $\alpha(T)$ [in $\mu SV^{-1}T^{-1}$] defined in Eq. (1) as a function of temperature in double-logarithmic scales.

several limits of interest. First, one recognizes an oscillatory dependence on the doping level $\mu = vk_F$ tuned by a backgate voltage, similar to what is seen experimentally [10]. Second, $\alpha(T)$ [see Eq. (1)] is exponentially small for $\tilde{T} \gg 1$ but shows power-law scaling $\alpha(\tilde{T} \ll 1) \propto \tilde{T}^{2K-2}$ at low temperatures, implying a huge increase in $\alpha(T)$ when lowering T. Third, in the zero-temperature limit, Eq. (12) yields

$$I_e(\tilde{V}) \propto \sin[\delta(1 - K^2)\tilde{V}/K] \, \tilde{V}^{K-1/2} J_{K-1/2}(\tilde{V}) \quad (14)$$

with the Bessel function J_ν [26]. This implies the low-voltage scaling $I_e \propto \tilde{V}^{2K}$, *a posteriori* justifying our perturbative treatment of the impurity potential. Remarkably, I_e shows *oscillatory behavior* as a function of the bias voltage V. As one can see from Eq. (14), there are two different oscillation periods,

$$\Delta V_1 = \frac{2\pi \hbar v}{eKL}, \quad \Delta V_2 = \frac{K\Delta V_1}{\delta(1 - K^2)}. \quad (15)$$

For strong interactions, ΔV_2 can in principle provide direct information about δ. In any case, ΔV_1 should be readily observable and yields already the Luttinger parameter K. Inspection of Eq. (10) suggests that the physical reason for these oscillations is the quantum interference between right- and left-moving waves travelling between the two impurities with different velocities.

Let us then go back to the full four-channel case, and perform the integration in Eq. (10) numerically. To be specific, we consider a long and adiabatically connected $(10,4)$ SWNT with two symmetric impurities separated by $L = 20$ nm. Fig. 1 shows I_e as a function of V for several T. Oscillatory behaviors with bias voltage are clearly visible. With decreasing temperature, I_e increases and one gets power-law scaling of $\alpha(T) \propto T^{(K-1)/2}$ at low T (see inset of Fig. 1), generalizing the above single-channel result. Notably, $\alpha(T)$ has the same sign for a given parameter set, in qualitative agreement with experiments

[10]. Within our parameter choices, also the order of magnitude in $\alpha(T)$ agrees with Ref. [10]. In any case, the picture obtained in the single-channel version is essentially recovered under the four-channel calculation.

To conclude, we have analyzed nonlinear magnetochiral transport properties of interacting single-wall carbon nanotubes. In chiral tubes, measurement of the odd-in-B component I_e (which must be even in V) provides direct information about interactions and chirality not accessible otherwise. For two impurities, we have presented detailed analytical results for I_e. We predict oscillations of I_e as a function of bias voltage, which provide direct information about the interaction parameter K. More-over, at low temperatures, power-law scaling is found and leads to an enhancement of I_e. In future work, our approach should be useful when calculating fluctuations of transport coefficients in disordered interacting SWNTs.

[1] M. Bockrath, D.H. Cobden, J. Lu, A.G. Rinzler, R.E. Smalley, L. Balents, and P.L. McEuen, Nature (London) **397**, 598 (1999); Z. Yao, H.W.C. Postma, L. Balents, and C. Dekker, Nature (London) **402**, 273 (1999); B. Gao, A. Komnik, R. Egger, D.C. Glattli, and A. Bachtold, Phys. Rev. Lett. **92**, 216804 (2004).

[2] R. Egger and A.O. Gogolin, Phys. Rev. Lett. **79**, 5082 (1997); Eur. Phys. J. B **3**, 281 (1998); C. Kane, L. Balents, and M.P.A. Fisher, Phys. Rev. Lett. **79**, 5086 (1997).

[3] T. Ando, J. Phys. Soc. Jpn. **74**, 777 (2005).

[4] For a (n, m) SWNT, the chiral angle is $\theta = \tan^{-1}[\sqrt{3}m/(2n + m)]$. The (n, m) indices determine whether the SWNT is metallic or semiconducting [3].

[5] L. Onsager, Phys. Rev. **38**, 2265 (1931); H.B.G. Casimir, Rev. Mod. Phys. **17**, 343 (1945); M. Büttiker, Phys. Rev. Lett. **57**, 1761 (1986).

[6] G.L.J.A. Rikken, J. Fölling, and P. Wyder, Phys. Rev. Lett. **87**, 236602 (2001).

[7] E.L. Ivchenko and B. Spivak, Phys. Rev. B **66**, 155404 (2002).

[8] D. Sánchez and M. Büttiker, Phys. Rev. Lett. **93**, 106802 (2004); B. Spivak and A. Zyuzin, Phys. Rev. Lett. **93**, 226801 (2004); M.L. Polianski and M. Büttiker, Phys. Rev. Lett. **96**, 156804 (2006); E. Deyo, B. Spivak, and A. Zyuzin, cond-mat/0603731.

[9] V. Krstic, S. Roth, M. Burghard, K. Kern, and G.L.J.A. Rikken, J. Chem. Phys. **117**, 11 315 (2002).

[10] J. Wei, M. Shimogawa, Z. Wang, I. Radu, R. Dormaier, and D.H. Cobden, Phys. Rev. Lett. **95**, 256601 (2005).

[11] A. Löfgren, C.A. Marlow, I. Shorubalko, R.P. Taylor, P. Omling, L. Samuelson, and H. Linke, Phys. Rev. Lett. **92**, 046803 (2004).

[12] C.A. Marlow, R.P. Taylor, M. Fairbanks, I. Shorubalko, and H. Linke, Phys. Rev. Lett. **96**, 116801 (2006).

[13] R. Leturcq, D. Sánchez, G. Götz, T. Ihn, K. Ensslin, D.C. Driscoll, and A.C. Gossard, Phys. Rev. Lett. **96**, 126801 (2006).

[14] D.M. Zumbühl, C.M. Marcus, M.P. Hanson, and A.C. Gossard, Phys. Rev. Lett. **96**, 206802 (2006).

[15] L. Angers, E. Zakka-Bajjani, R. Deblock, S. Gueron, H. Bouchiat, A. Cavanna, and U. Gennser, cond-mat/0603303.

[16] A.O. Gogolin, A.A. Nersesyan, and A.M. Tsvelik, *Bosonization and Strongly Correlated Systems* (Cambridge University Press, Cambridge, 1998).

[17] Fermi momenta are also slightly different for R/L movers and/or in different bands. For a calculation of I_e, this is inessential and neglected henceforth.

[18] C.L. Kane, E.J. Mele, A.T. Johnson, D.E. Luzzi, B.W. Smith, D.J. Hornbaker, and A. Yazdani, Phys. Rev. B **66**, 235423 (2002).

[19] P.L. McEuen, M. Bockrath, D.H. Cobden, Y.-G. Yoon, and S.G. Louie, Phys. Rev. Lett. **83**, 5098 (1999).

[20] Electron-electron backscattering effects in SWNTs are tiny [2] and disregarded here.

[21] R. Egger and H. Grabert, Phys. Rev. B **58**, 10761 (1998).

[22] This is also relevant for spin-orbit coupled quantum wires, see A. De Martino and R. Egger, Europhys. Lett. **56**, 570 (2001).

[23] D. Sánchez and M. Büttiker, Phys. Rev. B **72**, 201308(R) (2005).

[24] H.W.Ch. Postma, T. Teepen, Z. Yao, M. Grifoni, and C. Dekker, Science **293**, 76 (2001).

[25] For the one-channel case, I_e follows from Eq. (9) by multiplying by $1/4$, and by replacing $e^{i\pi \mathcal{G}^<} \to e^{i4\pi G^<}$.

[26] I.S. Gradshteyn and I.M. Ryzhik, *Table of Integrals, Series, and Product* (Academic Press, Inc., 1980).